Lüttinger Liquid Theory as a Model of the Gigahertz Electrical Properties of Carbon Nanotubes

P. J. Burke

Abstract—We present a technique to directly excite Lüttinger liquid collective modes in carbon nanotubes at gigahertz frequencies. By modeling the nanotube as a nano-transmission line with distributed kinetic and magnetic inductance as well as distributed quantum and electrostatic capacitance, we calculate the complex frequency-dependent impedance for a variety of measurement geometries. Exciting voltage waves on the nano-transmission line is equivalent to directly exciting the yet-to-be observed one-dimensional plasmons, the low energy excitation of a Lüttinger liquid. Our technique has already been applied to two-dimensional plasmons and should work well for one-dimensional plasmons. Tubes of length 100 microns must be grown for gigahertz resonance frequencies. Ohmic contact is not necessary with our technique; capacitive contacts can work. Our modeling has applications in potentially Terahertz nanotube transistors and RF nanospintronics.

Index Terms—Nanoelectronics, nanotechnology, nanotube, nanowire, spintronics.

I. INTRODUCTION

ONE OF THE MOST fundamental unsolved questions in modern condensed matter physics is: What is the ground state of a set interacting electrons, and what are the low-lying excitations? By far the most successful theoretical treatment of interactions is Landau's theory of Fermi liquids, which posits that the low-lying excitations of a Fermi liquid are not in fact electrons, but "quasi-particles" which, to good approximation, are noninteracting. The reason that the quasi-particles can be treated as noninteracting is that the inverse quantum lifetime of a quasi-particle is generally less than its energy, so that the concept of an independent quasi-particle is well defined. Landau's Fermi liquid theory has served physicists well in two and three dimensions for many decades. Unfortunately, it has long been known that Landau's Fermi liquid theory breaks down in one-dimensional (1-D) systems [1], such as those formed in single-walled carbon nanotubes (SWNTs) [2].

To deal with this problem, Tomonaga [3], and later Lüttinger [4], described a simplified model for interacting electrons in one dimension, which was exactly solvable. The method used was that of bosonization [5], [6]. The boson variables describe collective excitations in the electron gas, called *1-D plasmons*. Later, Haldane [7] argued that the bosonization description was generically valid for the low energy excitations of a 1-D system of interacting electrons, coining the term the "Lüttinger liquid."

In this model, the creation of an electron is equivalent to exciting an infinite number of 1-D plasmons. Much theoretical work [1] has gone into calculating the experimental consequences of the non-Fermi liquid behavior of 1-D systems. The main experimental consequences calculated and observed [8] to date are the power-law dependence of conductivity on temperature and the power-law dependence of tunneling current on bias voltage, when the contact of three-dimensional (3-D) macroscopic leads to the 1-D system is through high resistance tunnel barriers. The power-law exponent is generally characterized by a dimensionless parameter "g." For noninteracting electrons, $g = 1$, while for interacting electrons, $g < 1$. To date, the experimental evidence for the theory that the low-lying excitations of interacting electrons in one dimension are collective plasmon oscillations, while significant, is somewhat indirect.

It is the purpose of this paper to describe a technique that can be used to directly excite the 1-D plasmons using a microwave signal generator. (Similar proposals have appeared in the literature already [9]–[11].) This technique was recently applied to measure collective oscillations (plasmons) in a two-dimensional (2-D) electron gas, including measurements of the 2-D plasmon velocity, as well as the temperature and disorder dependent damping [12]. Our goal in this paper is to describe a technique to extend these measurements to one-dimensional systems, and to discuss a method to directly measure the 1-D plasmon velocity, and hence "g" in a Lüttinger liquid. In order to discuss this technique, one of our goals in this paper is to provide an effective circuit model for the effective electrical [dc to gigahertz to terahertz] properties 1-D interacting electron systems. While we restrict our attention to metallic SWNTs, the general approach can be used to describe semiconducting carbon nanotubes, multiwalled carbon nanotubes, quantum wires in GaAs heterostructures [13], and any other system of 1-D interacting electrons.

In our recent 2-D plasmon work, we suggested a transmission-line effective circuit model to relate our electrical impedance measurements to the properties of the 2-D plasmon collective excitation [12], [14]–[16]. There, we measured the kinetic inductance of a 2-D electron gas, as well as its distributed electrostatic capacitance to a metallic "gate" by directly exciting it with a microwave voltage. The distributed capacitance and inductance form a transmission line, which is an electrical engineer's view of a 2-D plasmon.

Since then, the transmission-line description has been discussed in the context of both single-walled [17] and multiwalled [18], [19] carbon nanotubes. In [17], by considering the Lagrangian of a 1-D electron gas (1-DEG), an expression for the *distributed* quantum capacitance (which was not important in

our 2-D experiments) as well as the *distributed* kinetic inductance of a SWNT is derived. (In [20] and [21], the concept of a lumped (as opposed to distributed) quantum capacitance and quantum/kinetic inductance is introduced.) In [18], [19] the tunnel conductance at high voltages is related to electrical parameters (the characteristic impedance) of the transmission line in a multiwalled nanotube. In both of these discussions, the distributed inductance and capacitance per unit length form a transmission line, which is again an electrical engineer's description of a 1-D plasmon. It is the goal of this manuscript to describe how we can excite 1-D plasmons directly with a microwave voltage, calculate the expected results for a variety of possible measurement geometries (including capacitive as well as tunneling electrical contacts), and discuss how our technique can be used to directly measure the Lüttinger liquid parameter "g."

We proceed as follows. First, we rederive the results of reference [17] for a spinless 1-D quantum wire, by calculating the kinetic inductance, electrostatic capacitance, and quantum capacitance per unit length. We extend the results of [17] by considering the magnetic inductance per unit length, as well as the characteristic impedance. We then proceed to discuss spin-1/2 electrons in an SWNT, and derive four coupled equations for the voltages on each of the four quantum channels in an SWNT, following [19]. We diagonalize these equations of motion and solve for the spin/charge modes. These results are not meant to be rigorous many-body calculations, but a way to translate theoretical ideas about interacting electrons in one dimension into measurable predictions. For more rigorous discussions, the reader is referred to [9]–[11] and [20]–[23].

In Section II of this paper, we proceed to discuss our technique to directly excite these 1-D plasmons by setting up standing-wave resonances in SWNTs of finite length, as we did in the 2-D plasmon case. We calculate explicitly measurable electronic properties of 1-D plasmons that are amenable to the measurement technique we developed for 2-D plasmons, including the nanotube dynamical impedance (real and imaginary) as a function of frequency, as well as the 1-D plasmon damping, wave velocity, and Lüttinger "g" factor. We discuss what experimental parameters are needed to perform our experiment, and also how the low (sub-GHz) frequency properties of nanotubes may be used to give some insight into the 1-D plasmon. Finally, we discuss possible practical consequences [24] of the results in nanotube electronic and micro/nano-mechanical high-frequency circuits. Our measurement technique could provide direct evidence for collective mode behavior of interacting electrons in one dimension, the "Lüttinger liquid."

II. CIRCUIT MODEL FOR SPINLESS ELECTRONS IN A ONE-CHANNEL QUANTUM WIRE

The dc circuit model for a one-channel quantum wire of noninteracting electrons is well known from the Landauer–Büttiker formalism of conduction in quantum systems. The dc conductance is simply given by e^2/h. If the spin degree of freedom is accounted for, there are two "channels" in a quantum wire: spin up and spin down, both in parallel. We postpone our discussion of spin until the next section, and assume for the moment the
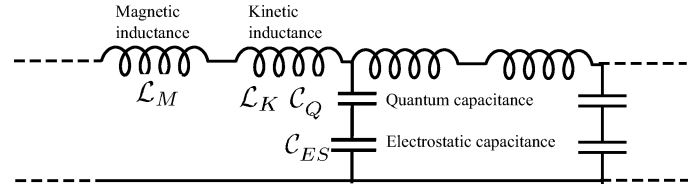

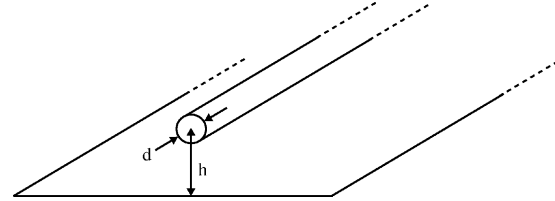Fig. 1. Circuit diagram for 1-D system of spinless electrons. Symbols are defined per unit length.

Fig. 2. Geometry of nanotube in presence of a ground plane.

electrons are spinless. At ac, the circuit model is not well established experimentally. However, theoretically it is believed to be equivalent to a transmission line, with a distributed "quantum" capacitance and kinetic inductance per unit length. It is generally believed [1] that the effect of electron-electron interactions can be included in the transmission line circuit analogy as an electrostatic capacitance. Furthermore, there will also be a magnetic inductance.

The effective circuit diagram we are proposing is shown in Fig. 1. Below, we will discuss each of the four contributions to the total circuit, and then discuss some of its general properties, such as the wave velocity and characteristic impedance. We will restrict ourselves to the case of a wire over a "ground plane" for the sake of simplicity. If there is no ground plane, the parameter "h" (the distance from the wire to the ground plane) should be replace by the length of the 1-D wire itself. The geometry we consider is shown in Fig. 2.

A. Magnetic Inductance

In the presence of a ground plane, the magnetic inductance per unit length is given by [25]

$$\mathcal{L}_M = \frac{\mu}{2\pi}\cosh^{-1}\left(\frac{2h}{d}\right) \approx \frac{\mu}{2\pi}ln\left(\frac{h}{d}\right) \qquad (1)$$

where d is the nanotube diameter and h is the distance to the "ground plane." The approximation is good to within 1% for $h > 2d$. This is calculated using the standard technique of setting the inductive energy equal to the stored magnetic energy

$$\frac{1}{2}LI^2 = \frac{1}{2\mu}\int B(x)^2 d^3x \qquad (2)$$

and using the relationship between I and B in the geometry of interest, in this case a wire on top of a ground plane. For a typical experimental situation, the nanotube is on top of an insulating (typically oxide) substrate, with a conducting medium below. (The finite conductivity of the conducting medium will be discussed below.) A typical oxide thickness is between 100 Å and 1 μm, whereas a typical nanotube radius is 1 nm. Because the

numerical value of $\mathcal{L}_M$ is only logarithmically sensitive to the ratio of d/h, we can estimate it within a factor of three as

$$\mathcal{L}_M \approx 1\,\mathrm{pH}/\mu\mathrm{m}. \tag{3}$$

We use μm for our length units because modern growth processes produce nanotubes with lengths of order micrometers and not (as of yet) meters.

B. Kinetic Inductance

In order to calculate the kinetic inductance per unit length, we follow [17] and calculate the kinetic energy per unit length and equate that with the $(1/2)LI^2$ energy of the kinetic inductance. The kinetic energy per unit length in a 1-D wire is the sum of the kinetic energies of the left-movers and right-movers. If there is a net current in the wire, then there are more left-movers than right-movers, say. If the Fermi level of the left-movers is raised by $e\Delta\mu/2$, and the Fermi-level of the right-movers is decreased by the same amount, then the current in the 1-D wire is $I = e^2/h\Delta\mu$. The net increase in energy of the system is the excess number of electrons ($N = e\Delta\mu/2\delta$) in the left versus right moving states times the energy added per electron $e\Delta\mu/2$. Here δ is the single particle energy level spacing, which is related to the Fermi velocity through $\delta = \hbar v_F 2\pi/L$. Thus, the excess kinetic energy is given by $hI^2/4v_F e^2$. By equating this energy with the $(1/2)LI^2$ energy, we have the following expression for the kinetic energy per unit length:

$$\mathcal{L}_K = \frac{h}{2e^2 v_F}. \tag{4}$$

The Fermi velocity for graphene and also carbon nanotubes is usually taken as $v_F = 8\ 10^5 m/s$, so that numerically

$$\mathcal{L}_K = 16\,\mathrm{nH}/\mu\mathrm{m}. \tag{5}$$

It is interesting to compare the magnitude of the kinetic inductance to the magnetic inductance. From (1) and (4), we have

$$\frac{\mathcal{L}_M}{\mathcal{L}_K} = \alpha \frac{2}{\pi} \frac{v_F}{c} \ln\left(\frac{h}{d}\right) \sim 10^{-4} \tag{6}$$

where $\alpha \approx 1/137$ is the fine structure constant. Thus, in 1-D systems, the kinetic inductance will always dominate. This is an important point for engineering nano-electronics: In engineering macroscopic circuits, long thin wires are usually considered to have relatively large (magnetic) inductances. In the case of nano-wires, the magnetic inductance is not that important; it is the kinetic inductance that dominates.

C. Electrostatic Capacitance

The electrostatic capacitance between a wire and a ground plane as shown in Fig. 2 is given by [25]

$$\mathcal{C}_E = \frac{2\pi\epsilon}{\cosh^{-1}(2h/d)} \approx \frac{2\pi\epsilon}{\ln(h/d)} \tag{7}$$

where again the approximation is good to within 1% for $h > 2d$. This can be approximated numerically as

$$\mathcal{C}_E \approx 50\,\mathrm{aF}/\mu\mathrm{m}. \tag{8}$$

This is calculated using the standard technique of setting the capacitive energy equal to the stored electrostatic energy

$$\frac{Q^2}{2C} = \frac{\epsilon}{2} \int E(x)^2 d^3x \tag{9}$$

and using the relationship between E and Q in the geometry of interest, in this case a wire on top of a ground plane. The term "electrostatic" comes from the approximation that we make in calculating the capacitance using (9), which is done using the relationship between a static charge and a static electric field. However, the electrostatic capacitance can of course be used when considering time-varying fields, voltages, currents, and charges, as we will do below.

D. Quantum Capacitance

In a classical electron gas (in a box in one, two, or three dimensions), to add an extra electron costs no energy. (One can add the electron with any arbitrary energy to the system.) In a quantum electron gas (in a box in one, two, or three dimensions), due to the Pauli exclusion principle it is not possible to add an electron with energy less than the Fermi energy E_F. One must add an electron at an available quantum state above E_F. In a 1-D system of length L, the spacing between quantum states is given by

$$\delta E = \frac{dE}{dk}\delta k = \hbar v_F \frac{2\pi}{L} \tag{10}$$

where L is the length of the system, and we have assumed a linear dispersion curve appropriate for carbon nanotubes. By equating this energy cost with an effective quantum capacitance [11], [17], [18] with energy given by

$$\frac{e^2}{C_Q} = \delta E \tag{11}$$

one arrives at the following expression for the (quantum) capacitance per unit length:

$$\mathcal{C}_Q = \frac{2e^2}{h v_F} \tag{12}$$

which comes out to be numerically

$$\mathcal{C}_Q = 100\,\mathrm{aF}/\mu\mathrm{m}. \tag{13}$$

The ratio of the electrostatic to the quantum capacitance is then given by

$$\frac{\mathcal{C}_{ES}}{\mathcal{C}_Q} = \frac{2\pi h}{e^2 \mu v_F} \ln\left(\frac{h}{d}\right) = \frac{1}{\alpha}\frac{2}{\pi}\frac{v_F}{c}\ln\left(\frac{h}{d}\right) \sim 1. \tag{14}$$

Thus, when considering the capacitive behavior of nano-electronic circuit elements, both the quantum capacitance and the electrostatic capacitance must be considered.

E. Wave Velocity

For a distributed inductance and capacitance per unit length, a technique used by theorists is to write down the Lagrangian (kinetic minus potential energy), and then to use the Euler–Lagrange equations to derive an equation of motion which, in this case, ends up being a wave equation. However, a much simpler

(if somewhat less rigorous) approach is simply to use a result known by RF engineers for many decades, namely, that the wave velocity of a circuit with distributed inductance and capacitance is given by

$$v_{\text{general}} = \sqrt{\frac{1}{\mathcal{L}\mathcal{C}}}. \tag{15}$$

If we consider only the magnetic inductance (neglecting the kinetic inductance) and if we also consider only the electrostatic capacitance (neglecting the quantum capacitance), then the wave velocity would simply by the speed of light c

$$v_{\text{freespace}} = \sqrt{\frac{1}{\mathcal{L}_M \mathcal{C}_{ES}}} = \sqrt{\frac{1}{\mu\epsilon}} = c. \tag{16}$$

A full solution to the collective mode of a carbon nanotube should include both the kinetic inductance as well as the magnetic inductance, which we write as

$$\mathcal{L}_{\text{total}} = \mathcal{L}_K + \mathcal{L}_M \tag{17}$$

as well as both the quantum capacitance and the electrostatic capacitance, which we write as

$$\mathcal{C}_{\text{total}}^{-1} = \mathcal{C}_Q^{-1} + \mathcal{C}_{ES}^{-1}. \tag{18}$$

In our recent work [12] on a two-dimensional electron gas system (in the presence of a ground plane), we found that the kinetic inductance dominates $\mathcal{L}_{\text{total}}$, and that the geometric capacitance dominates $\mathcal{C}_{\text{total}}$, so that the collective mode velocity in two dimensions is given by

$$v_{2-D} \approx \sqrt{\frac{1}{\mathcal{L}_K \mathcal{C}_{ES}}}. \tag{19}$$

However, as our estimates above show, for a 1-D quantum system such as a nanotube, the quantum capacitance is predicted to dominate $\mathcal{C}_{\text{total}}$, so that in one dimension we have the approximation that

$$v_{1-D,\text{noninteracting}} \approx \sqrt{\frac{1}{\mathcal{L}_K \mathcal{C}_Q}} = v_F. \tag{20}$$

One method of including the effect of electron–electron interactions in the context of the above discussion is simply to include the electrostatic capacitance as well as the quantum capacitance, so that the wave velocity is not quite exactly equal to the Fermi velocity

$$v_{1-D,\text{interacting}} \approx \sqrt{\frac{1}{\mathcal{L}_K \mathcal{C}_{\text{total}}}} = \sqrt{\frac{1}{\mathcal{L}_K \mathcal{C}_{ES}} + \frac{1}{\mathcal{L}_K \mathcal{C}_Q}} > v_F. \tag{21}$$

The ratio of the plasmon velocity in the presence of interactions to the plasmon velocity in the absence of interactions has a special significance, and it is given in this simple model by

$$g_{\text{spinless}} \equiv \frac{v_F}{v_{1-D,\text{interacting}}} = \left(1 + \frac{\mathcal{C}_Q}{\mathcal{C}_{ES}}\right)^{-1/2}$$
$$= \left(1 + \alpha \frac{\pi}{2} \frac{c}{v_F} \frac{1}{\ln(h/d)}\right)^{-1/2}. \tag{22}$$

(We use the subscript spinless to differentiate g_{spinless} from a different g which we define below.) This immediately suggests a technique to search for Lüttinger liquid behavior in order to measure g_{spinless}, namely, to measure the wave velocity. According to these calculations, the measured wave velocity should differ from the Fermi velocity by a large factor, of order unity. (If the distance to the ground plane becomes larger than the tube length such as in some free-standing carbon nanotubes [26], another formula for the capacitance has to be used, which involves replacing h with the length of the 1-D wire.) Finally, we note that the full solution to the wave velocity is given by

$$v_{1-D,\text{interacting}} = \sqrt{\frac{1}{\mathcal{L}_{\text{total}}\mathcal{C}_{\text{total}}}}$$
$$= \sqrt{\frac{1}{(\mathcal{L}_K + \mathcal{L}_M)}\left(\frac{1}{\mathcal{C}_Q} + \frac{1}{\mathcal{C}_{ES}}\right)}$$
$$= v_F \sqrt{\frac{1 + \alpha \frac{\pi}{2} \frac{c}{v_F} \ln(d/h)}{1 + \alpha \frac{2}{\pi} \frac{v_F}{c} \ln(h/d)}}. \tag{23}$$

With this, the g factor should read

$$g_{\text{spinless}} = \left(\frac{1 + \alpha \frac{\pi}{2} \frac{c}{v_F} \ln(d/h)}{1 + \alpha \frac{2}{\pi} \frac{v_F}{c} \ln(h/d)}\right)^{-1/2}. \tag{24}$$

To our knowledge this full function has not been discussed in the literature. We speculate that g_{spinless} should be redefined as in (24) to include this term, which is equivalent to adding the magnetic energy term to the Hamiltonian.

The definition of g in a quantum wire when the spin degree of freedom is taken into account will be discussed in further detail below. For now, we would like to address the question which naturally arises in the context of this discussion, how to observe these collective excitations? One technique, which we propose here, is to measure the wave velocity in the frequency or time domain. To date these collective excitations have been observed by one other experimental technique, namely, that of tunneling. Using a further set of calculations [1], it can be shown that the tunneling density of states is modified, which gives rise to testable predictions to experimental tunneling I–Vs. For the case of the I–V curve of a single tunnel-contacted nanotube, the model is that there is a 3-D–1-D tunneling interface of sorts as the "ohmic contact" of one end of the tube, and a 1-D–3-D tunneling interface at the other "ohmic contact." Experiments have observed [8] power-law behavior that is consistent with the tunneling predictions, namely $dI/dV \propto V^\alpha$, where $\alpha = (g^{-1} - 1)/4$ or $\alpha = (g^{-1} + g - 2)/8$, depending on whether the contact is at the end or in the bulk of the tube. In the 3-D–1-D tunneling case, an electron tunnels into the 1-D system, which simultaneously excites an infinite number of 1-D plasmons. In reference [8], experimentally observed values of α vary between 0.33–0.38 for end-tunneling, and 0.5–0.7 for bulk tunneling, giving values of g between 0.26–0.33. A recent paper [13] also measured tunneling from one 1-D quantum wire in GaAs to another 1-D quantum wire in GaAs. There, they found $g \approx 0.75$. Both of these approaches are interesting and significant.

In this manuscript we would like to present a different and complementary method to measure these collective excitations

directly, by exciting them with a microwave (GHz) voltage. In particular, we would like to measure the wave velocity under a variety of conditions, including different distances from the nanotube to the ground plane, to see how the electromagnetic environment effects the properties of collective excitations in 1-D quantum systems. An additional capability of the technique described below would be to measure the 1-D plasmon damping, including dependence on temperature and disorder. This high-frequency measurement may also have direct applications in determining the switching speed of a variety of nanotube based electronic devices.

F. Characteristic Impedance

Another property of interest of the transmission line is the characteristic impedance, defined as the ratio of the ac voltage to the ac current. This is especially important for measurement purposes. In the circuit model presented above, for a right-going plasmon wave, the ratio of the ac voltage to the ac current is independent of position, and is given by

$$Z_{c,\text{general}} = \sqrt{\frac{\mathcal{L}}{\mathcal{C}}}. \tag{25}$$

As we did for the wave velocity, we have to consider the magnetic and kinetic inductance, as well as the electrostatic and quantum capacitance. Upon considering the magnetic and electrostatic inductance only, one recovers the characteristic impedance of free space

$$Z_{c,\text{freespace}} = \sqrt{\frac{\mathcal{L}_M}{\mathcal{C}_{ES}}} = \sqrt{\frac{\mu}{\epsilon}} \equiv Z_0 = 377\,\Omega. \tag{26}$$

On the other hand, if one considers only the quantum capacitance and only the kinetic inductance, the characteristic impedance turns out to be the resistance quantum

$$Z_{c,\text{noninteracting,spinless}} = \sqrt{\frac{\mathcal{L}_K}{\mathcal{C}_Q}} = \frac{h}{2e^2} = 12.5\,\text{k}\Omega. \tag{27}$$

Now, if one considers the kinetic inductance and both components of the capacitance (electrostatic + quantum), then one finds

$$
\begin{aligned}
Z_{c,\text{interacting,spinless}} &= \sqrt{\frac{\mathcal{L}_K}{\mathcal{C}_{\text{total}}}} = \sqrt{\frac{\mathcal{L}_K}{\mathcal{C}_{ES}} + \frac{\mathcal{L}_K}{\mathcal{C}_Q}} \\
&= \sqrt{\frac{\mathcal{L}_K}{\mathcal{C}_Q}} \left(1 + \alpha \frac{\pi}{2} \frac{c}{v_F} \frac{1}{\ln(h/d)} \right)^{1/2} \\
&= g_{\text{spinless}}^{-1} \frac{h}{2e^2}
\end{aligned}
\tag{28}
$$

where we have inserted the definition of g_{spinless}. This immediately suggests a second method of measuring g at GHz frequencies, by measuring the characteristic impedance of the transmission line. We discuss the geometries of interest in detail in a later section. For now we would like to comment that, even though the characteristic impedance measurement at high frequencies of high resistances is challenging, the predicted variation of the characteristic impedance from the noninteracting $h/2e^2$ is large, of order 100%.

To be complete, we must include the magnetic inductance as well, yielding the full solution to the characteristic impedance

$$
\begin{aligned}
Z_{c,\text{total,spinless}} &= \sqrt{\frac{\mathcal{L}_{\text{total}}}{\mathcal{C}_{\text{total}}}} \\
&= \sqrt{(\mathcal{L}_K + \mathcal{L}_M) \left(\frac{1}{\mathcal{C}_Q} + \frac{1}{\mathcal{C}_{ES}} \right)} \\
&= \frac{h}{2e^2} \sqrt{\left(1 + \alpha \frac{\pi}{2} \frac{c}{v_F} \frac{1}{\ln(h/d)} \right) \left(1 + \alpha \frac{2}{\pi} \frac{v_F}{c} \ln(h/d) \right)} \\
&= \frac{h}{2e^2} \sqrt{1 + \alpha \left(\frac{\pi}{2} \frac{c}{v_F} \frac{1}{\ln(h/d)} + \frac{2}{\pi} \frac{v_F}{c} \ln(h/d) \right) + \alpha^2}.
\end{aligned}
\tag{29}
$$

G. Intrinsic Damping Mechanisms?

An important question to consider is the damping of the 1-D plasma waves. Currently, very little is known theoretically or experimentally about the damping *mechanisms*. In the absence of such knowledge, we proceed phenomenologically in the following section. We model the damping as distributed resistance along the length of the tube. (This model of damping of 2-D plasmons we recently measured was successful in describing our experimental results, using the dc resistance to estimate the ac damping coefficient.) Unfortunately, to date, even the dc resistance of metallic nanotubes is not well quantified. What *is* known is that the scattering length at low temperatures is at least 1 μm, and possibly more. This is known from recent experiments where the tube length of 1 μm gave close to the Landauer–Büttiker theoretical resistance for the dc measurement, indicating ballistic (scatter free) transport over the length of the entire tube [27]. We state this clearly in an equation for the mean free path

$$l_{\text{m.f.p.}} > 1\,\mu\text{m}. \tag{30}$$

Now, for dynamical measurements one is usually concerned with the scattering rate, not length, so if we assume the relationship:

$$l_{\text{m.f.p.}} = v_F \tau \tag{31}$$

then we have

$$\tau > 1\,\text{ps}. \tag{32}$$

A separate recent measurement [28] of the millimeter-wave conductivity of mats of single-walled nanotubes gave a scattering time of 4 ps at room temperature, but it is unclear how that relates to the scattering time of individual nanotubes. The condition that must prevail for resonant geometries (see below) is that Q must be greater than one. This implies the condition

$$\omega\tau > 1. \tag{33}$$

For a 4-ps scattering time, this means the resonant frequency of any cavity must be greater than 40 GHz. However, we still do not have any data on how much greater the mean free path is than 1μm and, hence, the condition $\omega\tau > 1$ could be satisfied at frequencies below 1 GHz. (In fact an ac measurement of the impedance of a single nanotube could give more quantitative

information about the mean-free-path as well as the damping coefficient of 1-D plasmons.) We speculate that nanotubes with scattering times satisfying $\omega\tau > 1$ at frequencies below 1 GHz could be grown if they do not already exist; this would correspond to a mean free path of order 100 μm. We discuss the experimental consequences of this issue in the next section in more detail.

H. Damping From an External Circuit or Ground Plane

Another important damping mechanism is if the ground plane is not a perfect conductor. For a superconducting ground plane, the approximation of a perfect conductor is a good one. We discuss now two other cases of interest, that of a metallic film ground plane, and that of a doped semiconducting ground plane.

A typical deposited metal film will have a thickness of order 0.1 μm, which is much less than the skin depth at GHz frequencies. Hence, it can be treated as having a certain sheet resistance, which is typically of order 1 Ω per square at room temperature, although it might be substantially less at cryogenic temperatures. For the effective width of order a nanotube width that participates in the "grounding," this would give rise to a resistance per length $\mathcal{R}$ of the ground plane of order 1 kΩ/μm, which could be a significant source of damping, even if there is no scattering whatsoever within the nanotube itself. Plasma waves of frequencies below $1/2\pi\tau = \mathcal{R}/2\pi\mathcal{L} = 10$ GHz would be severely damped. If, instead of a thin film, a bulk metal is used, then the skin depth must be considered. In that case, the resistance per square must be replaced by $\rho/\delta_{\text{S.D.}}$, where ρ is the bulk resistivity and $\delta_{\text{S.D.}}$ the skin depth, which is typically 1 μm at 1 GHz in copper at room temperature. Thus, by increasing the thickness of the metallic ground plane to 1 μm, one can decrease the damping coefficient of the plasmons. However, going any thicker than the skin depth does not help. (Interestingly, the exact same principle applies to gold plating the conductors of coaxial cables: it is not necessary and certainly not economical to use bulk gold at RF frequencies for the cable material.) For a 1-μm-thick metal ground plane, then, the effective resistance per length that must be added to the transmission line circuit of the 1-D wire can be of order 100 Ω/μm, which is small but not insignificant.

For a doped-semiconductor ground plane, a typical bulk resistivity for an n-type doped Si wafer is 10 $\Omega \cdot$ cm. For this resistivity, the skin depth is of order 1 mm at 1 GHz, so that the effective resistance per square of the ground is given by 10 Ωcm/1 mm $= 100\,\Omega$ per square. This would give a resistance per unit length of order 100 kΩ/μm, which is a severe damping, much worse than any scattering in the nanotube itself. In this case, any plasmons with frequency below 1 THz would be heavily damped. However, when the skin depth is that large, corresponding to a distributed resistance in the "ground" plane that continues all the way down to 1 mm below the nanotube, the above calculations for the characteristic impedance and wave velocity (which implicitly assumed that the tube length was much larger than the distance to the ground plane) would have to be revised. We suspect that further numerical modeling is necessary to fully and quantitatively understand the interaction at GHz to THz frequencies between a nanotube and a doped

semiconducting gate, and its effect on damping of 1-D Lüttinger liquid plasmons.

The important point here is that, even if there is no scattering whatsoever in the nanotube itself, there may still be damping of the plasmon mode due to the electromagnetic coupling to the resistive ground plane.

One final possible loss mechanism is radiation into free space. This was implicitly neglected in calculating the capacitance using the electrostatic method [25]. The nano-tube can function as a nano-antenna, but since the wavelength of the radiation at GHz frequencies is of order cm, and the tube length is of order μm, it will not be a very efficient nano-antenna, so that radiation losses are not likely to be significant.

III. CIRCUIT MODEL FOR METALLIC SINGLE-WALL CARBON NANOTUBE

A carbon nanotube, because of its band structure, has two propagating channels, which we label as channel a and channel b [2]. In addition, the electrons can be spin up or spin down. Hence, there are four channels in the Landauer–Büttiker formalism language. In this section, we discuss an effective high-frequency circuit model which includes the contributions of all four channels, and makes the spin-charge separation (the hallmark of a Lüttinger liquid) clear and intuitive.

A. DC Spin-Charge Separation

For pedagogical reasons, let us first consider noninteracting spin 1/2 electrons in a single-mode quantum wire at dc. The current can be carried by either spin up or spin down electrons. Usually, when we measure the conductance of such a wire, the electrical contacts on both ends of the wire are to both the spin up and spin down channel simultaneously, so that the effective circuit model is two quantum channels in parallel. However, if we could inject current in one direction in the spin up channel, and extract current in the spin down channel, then the net electrical current (the *charge* current) would be zero. However, there would be a *spin* current. This clearly illustrates the separation of spin-charge currents in a 1-D wire at dc. Below, we consider the generalization to the ac case, and we consider a case where there are two modes for each spin orientation, correct for a carbon nanotube. We will neglect the magnetic inductance in what follows. Our approaches parallels that of reference [19], which in turn parallels that of reference [29]. We go further than these references, though, in diagonalizing and calculating the impedance matrix, and relating this to the *measurable* effective circuit impedance of a 1-D plasmon.

B. Noninteracting Circuit Model for Metallic Single-Wall Carbon Nanotube

The noninteracting ac circuit model of a single-walled carbon nanotube is fairly straightforward: We simply have four quantum channels in parallel each with its own kinetic inductance and quantum capacitance per unit length. (Neglecting the electrostatic capacitance is equivalent to neglecting the electron-electron interactions.) All of the above calculations would apply to that system, accept that there are four transmission lines in parallel. The ends of all four transmission lines
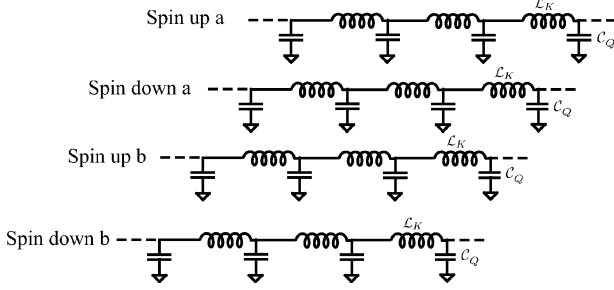
Fig. 3. Circuit model for noninteracting electrons in a single-walled carbon nanotube. Each channel (transmission line) is independent of the others.
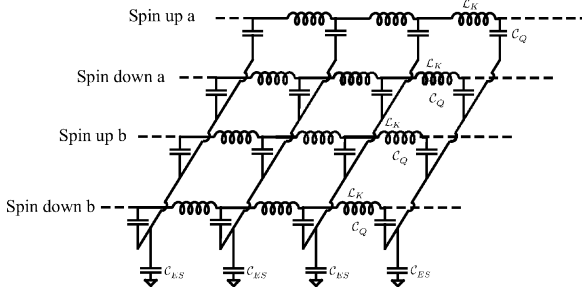

Fig. 4. AC circuit model for *interacting* electrons in a carbon nanotube.

are usually contacted simultaneously by electrical contacts to SWNTs. (Injecting spin-polarized current into only the spin up channels is another exciting possibility which we will explore in a future publication.) We draw in Fig. 3 the effective circuit diagram in this case.

C. Interacting Circuit Model for Metallic Single-Wall Carbon Nanotube

At this point, we have to take into account the electron–electron interaction. Apparently this can be done in a phenomenological way by using the electrostatic capacitance [30]. The coulomb energy per unit length is given by

$$E_c = \frac{(\rho_{\text{total}})^2}{2\mathcal{C}_{ES}} = \frac{1}{2\mathcal{C}_{ES}} \left(\sum_{i=1}^{4} \rho_i \right)^2$$
$$= \frac{1}{2\mathcal{C}_{ES}} (\rho_{a\uparrow} + \rho_{a\downarrow} + \rho_{b\uparrow} + \rho_{b\downarrow})^2 \quad (34)$$

where ρ_i is the charge per unit length in the ith mode. The circuit diagram of Fig. 4 takes this charging energy into account correctly, and is the central result of this paper.

At this point, we have a coupling between the four modes, which is immediately obvious in the circuit diagram in Fig. 4. Before we consider the formal mathematics, let us think about physically meaningful measurements. As in the dc case, if we apply an ac voltage to the nanotube, we are exciting all four channels simultaneously. (This is assuming the incoming current is not spin polarized, another exciting possibility we will not consider in this manuscript [31].) Therefore, at one end of the nanotube (the ground end) all four channels have zero voltage. At the other end of the nanotube (the "hot" end), all four channels have the same voltage V_0, for example. By inspection of the circuit diagram, the voltage along the nanotube will be the same for all four channels. This is actually a normal mode of the

coupled system, namely exciting all channels equally. It should also be obvious from inspecting the circuit diagram that there is no spin current in this case: as many spin up electrons move from right to left as spin down. As we will show below, there are three other normal modes which do not carry net current. Since they do not have net current flowing and they are called neutral modes. They do carry spin currents, though. Hence, the separation between spin and charge currents, which is one of the hallmarks of a Lüttinger liquid.

In the Appendix, we carry out this procedure mathematically, explicitly finding three spin modes (differential modes) and one charge mode (common mode) from the circuit diagram shown in Fig. 4. The charge mode is the common mode excitation of all four transmission lines in Fig. 4 We show in the Appendix that the charge-mode velocity is given by

$$v_p = \sqrt{\frac{1}{\mathcal{L}_K} \left(\frac{1}{\mathcal{C}_Q} + \frac{4}{\mathcal{C}_{ES}} \right)} = v_F \sqrt{1 + \frac{4\mathcal{C}_Q}{\mathcal{C}_{ES}}} \equiv v_F/g \quad (35)$$

where the last equality serves to define g for a SWNT. This result is not new [1], but the derivation based on our circuit model is. This derivation also provides a very clear and intuitive explanation of the spin-charge separation in a 1-D wire, which we discuss in Section III-D. We also show in the Appendix that the charge-mode characteristic impedance is given by

$$Z_{c,\text{C.M.}} \equiv \frac{V_{\text{C.M.}}^+}{I_{\text{C.M.}}^+} = -\frac{V_{\text{C.M.}}^-}{I_{\text{C.M.}}^-} = \sqrt{\frac{4\mathcal{L}_K}{\mathcal{C}_{ES}} + \frac{\mathcal{L}_K}{\mathcal{C}_Q}} = \frac{1}{g} \frac{h}{2e^2}. \quad (36)$$

We also show in the appendix that the velocity of the three spin modes (which we there call the differential modes) is given by

$$v_{\text{spin}} = v_F. \quad (37)$$

Thus, the spin modes and charge modes move at different velocities. We discuss the experimental consequences in Section IV.

D. AC Spin-Charge Separation: An Intuitive Explanation

Based on our transmission line description of a 1-D wire, we now give a simple description of the spin-charge separation of the ac excitations in a Lüttinger liquid. The *charge mode* corresponds to ac currents which flow simultaneously through spin-up and spin-down channels in the same direction. As a consequence, there is a local (dynamical) charging/discharging of the nanotube, and the electrostatic capacitance to the ground plane (as well as the quantum capacitance) is involved. Together with the distributed kinetic inductance, this gives the wave velocity of (35).

In contrast, the spin mode corresponds to ac spin up currents flowing in one direction, and ac spin down currents flowing in the *opposite* direction, i.e., out of phase by 180°. Since the spin-up and spin-down currents are always equal in magnitude but flowing in opposite directions, there is never any net charge buildup at any position along the nanotube. Thus, the electrostatic capacitance to the nearby gate is never charged up when the spin mode is excited, and is not relevant at all to the spin mode. For this reason, the spin mode is also referred to as the neutral mode. Of course, the distributed quantum capacitance

and the distributed kinetic inductance still are important, so that the spin mode is still an effective transmission line (i.e., the ac excitations are wavelike).

Since the electrostatic capacitance for the spin mode does not matter, the *wave velocity* (which is determined by the distributed inductance per unit length and the total capacitance per unit length) is different than the charge mode. The distributed capacitance per unit length for the charge mode consists of both the quantum *and* electrostatic capacitance, whereas for the spin mode it consists of only the quantum capacitance. The spin mode velocity *is* the Fermi velocity, and the charge mode velocity is g^{-1} times the Fermi velocity.

IV. MEASUREMENT TECHNIQUE

In this section, we consider various methods of exciting the common mode (charged) Lüttinger liquid plasmon with an ac voltage. In order to describe this, let us first consider measurements of the dc conductance of a single walled carbon nanotube. In the experiments performed to date, current flows through all four channels. In the case of tubes which approach $4e^2/h$ of conductance, i.e., where the macroscopic "lead" contacts all four channels, the current is equally distributed among all four channels. This is equivalent to exciting only the common-mode current, and the common-mode voltage as well. We would like to describe below a set of experiments where we contact all four channels simultaneously with an *ac* (microwave) voltage. This finite-frequency measurement will excite only the common-mode (charged) Lüttinger liquid 1-D plasmon. (In a future publication, we will discuss the possibility of driving microwave spin polarized current to excite the spin modes of the Lüttinger liquid.) Since there is a finite frequency, there will also be a wave vector introduced. If we measure the frequency dependent impedance of the nanotube, we should be able to determine the frequency at which there are one, two, three, etc., standing waves in the tube and, hence, measure the dispersion curve and wave velocity of the 1-D plasmon. From (35), this will allow a direct measurement of the parameter g.

In the appendix, we derived a set of differential equations describing the current and voltage for all four modes in a Lüttinger liquid (three neutral spin waves and one charge wave). Now, we would like to consider only the charged mode, and calculate the effective, frequency-dependent impedance that one would expect for a carbon nanotube at microwave frequencies.

At this point, we have two options. First, we can continue to work with the circuit diagram in Fig. 4, and apply the appropriate boundary conditions for the measurement geometries that we will consider below. This has the advantage that all four channels are still present in our effective circuit model, but it is somewhat complicated. However, for the boundary conditions this is actually a simpler option, as we will see.

Option two is to use the fact that we are considering only exciting the common mode in this paper, and to replace Fig. 4 with an "effective" circuit diagram consisting of a *single* transmission line with rescaled inductance and capacitance per unit length. This is indicated in Fig. 5, where the effective inductance per unit length is now $\mathcal{L}_K/4$, and the effective capacitance per unit length is given by $(\mathcal{C}_{ES}^{-1} + 4\mathcal{C}_Q^{-1})^{-1}$. The wave
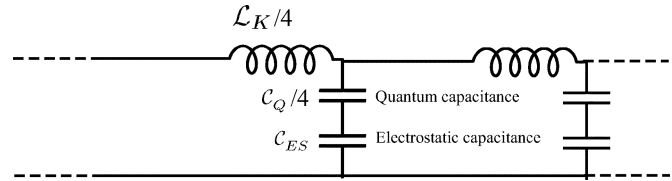

Fig. 5. Charge mode ("common mode") effective circuit diagram.

velocity of this "effective" circuit model is the same as the wave velocity of the common mode [given by (35)]. The characteristic impedance of this effective circuit model is 1/4 of the characteristic impedance of the common mode [given by (36)], which is due to the following. When we excite the common mode voltage, all four voltages $(V_{a,\uparrow}, V_{a,\downarrow}, V_{b,\uparrow}, V_{b,\downarrow})$ are *equal*, so that the common-mode voltage $V_{\text{C.M.}}$ is four times larger than the measured voltage by the external circuit, since $V_{\text{C.M.}} = V_{a,\uparrow} + V_{a,\downarrow} + V_{b,\uparrow} + V_{b,\downarrow}$ as given in (60). (The common-mode current is the same as the measured current.) The advantage of using the circuit diagram proposed in Fig. 5 is that we only have to deal with *one* transmission line. The disadvantage is that the effective boundary conditions for the geometries we consider below are not obvious and require careful consideration. In the following sections we will use both descriptions, according to convenience and relevance to the particular boundary conditions under consideration.

We proceed in this section as follows. We first consider an "ohmically" contacted nanotube, by which we mean tubes with dc electrical contacts with perfect transparency which have $4e^2/h$ of conductance. Of course, this is a linearized model of the dc resistance, which can have a significant nonlinear current–voltage relationship. It is beyond the scope of this paper to include nonlinear resistances in the effective circuit impedance. After considering "ohmically" contacted nanotubes, which are not trivial to achieve technologically, we consider a capacitively contacted nanotube which does not require dc contact. Such a measurement geometry should be much easier to achieve, since in essence it only requires evaporating a metal lead onto a nanotube, perhaps on top of a thin insulating barrier. A discussion of the measurement geometries requires careful consideration of the boundary conditions for the 1-D plasmons, which we treat below.

A. Ohmic Contacted Measurement

We begin by considering the simplest measurement geometry, that of an "ohmically" contacted single wall nanotube with perfect transparency at both ends. The dc conductance is just $4e^2/h$, since there are two channels and two spin orientations per channel. Tubes with dc resistance approaching this value have recently been fabricated [27]. For ac (dynamical) impedance measurements, we really do not know where to put the contact resistance in the ac circuit diagram. Experimentally, the high-frequency conductivity of nano-scale systems is an unexplored regime of mesoscopic physics; there have been few experiments [12], [32]–[35]. We speculate that the impedance can be modeled as a "contact" resistance, which is discussed more rigorously in reference [11], [36]. Following reference [11], we model the contact resistance as split into
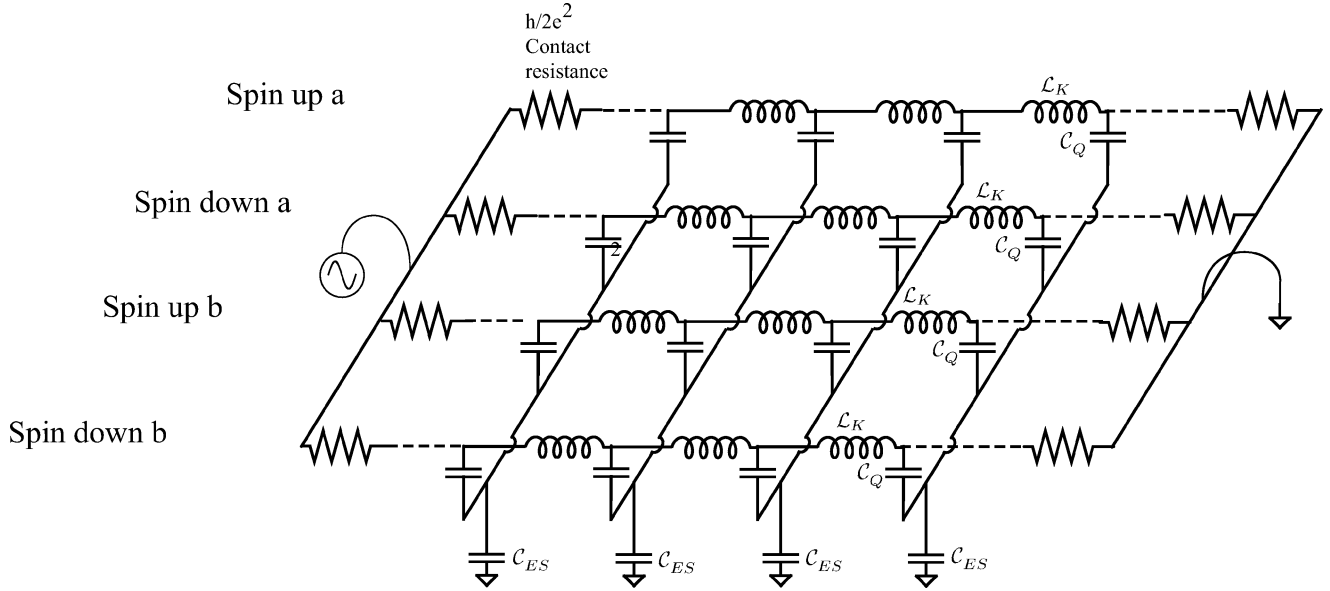
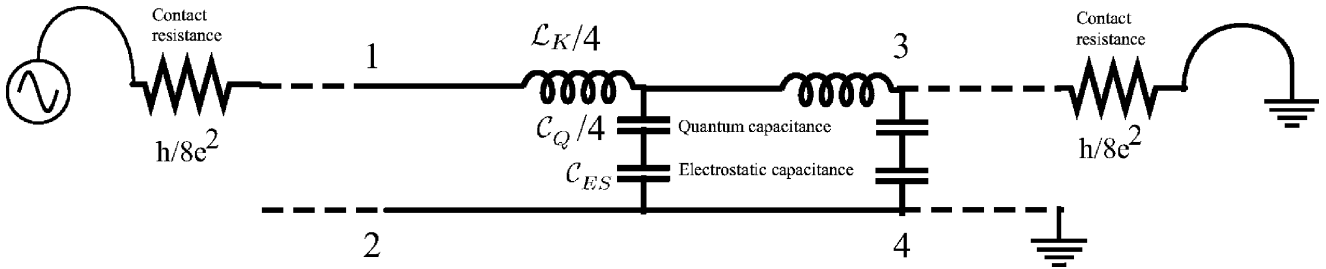Fig. 6. Circuit diagram for an SWNT with dc electrical contacts at both ends.

Fig. 7. *Effective* circuit diagram for an SWNT with dc electrical contacts at both ends.

a contact resistance ("charge relaxation resistance" [37]) on *each* side of the wire, so that each side has 1/2 of the total dc resistance. To be explicitly clear, we draw in Fig. 6 the circuit diagram we are proposing. At dc, each of the four channels has $h/2e^2 + h/2e^2 = h/e^2$ of total contact resistance. Since there are four quantum channels in parallel, the total resistance is given by $h/4e^2$, the Landauer–Büttiker expected value.

Now, it is possible to define an effective circuit diagram along the lines of Fig. 4. We show in Fig. 7 the effective circuit which is the "Norton equivalent" circuit to Fig. 6. The values for the contact resistance are shown as h/e^2 each. It is obvious from the circuit diagram that the dc resistance is equal to $h/4e^2$, so that our model is correct in the dc limit.

B. Ad Hoc, Phenomenological Damping Model

Before we continue, there is one more issue that needs to be discussed. That is the issue of damping along the length of the tube. We again speculate that the dc resistance per unit length gives information about the distributed damping of the 1-D plasmons. We model this as a distributed resistance per unit length $\mathcal{R}$. We must again be careful about the factor of four when we define this parameter. In our nomenclature, we define $\mathcal{R}$ as the dc resistance per unit length of all four channels in parallel. Of course, according to the scaling theory of localization [38], the resistance of a 1-D system is expected to scale exponentially

with length on the length scale of the localization length. However, it is known experimentally that the localization length is greater than a few micrometers, but it is not known how long the localization length really is. Our simplified model of a resistance per unit length violates the expected (but never observed) exponential scaling of the resistance with length in one dimension, but makes the problem tractable. According to our definition of $\mathcal{R}$ as the resistance per length of all four channels in parallel, we must insert a distributed resistance of $4\mathcal{R}$ into each of the channels in Fig. 6, or, equivalently, we must insert a resistance per unit length of $\mathcal{R}$ in the effective circuit diagram Fig. 7. Our discussion of damping in Section II-G is consistent with this definition. We will consider various numerical values of $\mathcal{R}$ below.

C. Impedance Calculations With Ohmic Contacts

At this point, we are in a position to calculate the (complex, frequency dependent) ratio of the ac voltage to the ac current entering the left end of the nanotube, the *impedance*. We do this by "mapping" the problem on to well-known problems in transmission line theory [39]. We proceed in two steps: First, we consider the impedance without the contact resistance on the left hand side. In other words, we calculate the impedance from point 1 in Fig. 7 to ground. This is equal to the impedance from point 1 to point 2 in Fig. 7, which is equivalent to the input

impedance of a (possibly lossy) transmission line with characteristic impedance $Z_{c,\text{effective}}$, which is "terminated" by a "load" impedance Z_L which in this case is simply the contact resistance, i.e. $Z_L = R_{\text{contact}} = h/8e^2$. This is a standard result in microwave theory, which we repeat here for convenience

$$Z_{in} = Z_{c,\text{effective}} \frac{1 + \Gamma e^{-2\gamma l}}{1 - \Gamma e^{-2\gamma l}} \tag{38}$$

where l is the length of the tube, and γ is the propagation constant of the 1-D plasmon, given by

$$\gamma \equiv \sqrt{(\mathcal{R} + i\omega \mathcal{L}_{\text{eff}})(i\omega \mathcal{C}_{\text{eff}})} \tag{39}$$

and where we have to defined $Z_{c,\text{effective}}$ as

$$Z_{c,\text{effective}} \equiv \sqrt{\frac{\mathcal{R} + i\omega \mathcal{L}_{\text{eff}}}{i\omega \mathcal{C}_{\text{eff}}}} \tag{40}$$

and where we have defined a new symbol Γ (the reflection coefficient of the plasmon wave off of the right end of load impedance "terminating" the nanotube) as

$$\Gamma \equiv \frac{Z_L - Z_{c,\text{effective}}}{Z_L + Z_{c,\text{effective}}}. \tag{41}$$

The effective inductance per unit length is

$$\mathcal{L}_{\text{eff}} \equiv \mathcal{L}_K/4 \tag{42}$$

and the effective capacitance per unit length is

$$\mathcal{C}_{\text{eff}}^{-1} \equiv 4\mathcal{C}_Q^{-1} + \mathcal{C}_{ES}^{-1} \tag{43}$$

as we have already indicated in Fig. 7. In the high frequency limit ($\omega > \mathcal{L}_{\text{eff}}/\mathcal{R}$), γ is just the wave vector k, i.e.

$$\lim_{\omega > \mathcal{R}/\mathcal{L}_{\text{eff}}} (\gamma) = k \equiv \frac{2\pi}{\lambda} = \frac{\omega}{v_p} \tag{44}$$

$$\lim_{\omega > \mathcal{R}/\mathcal{L}_{\text{eff}}} (Z_{c,\text{effective}}) = \frac{1}{g} \frac{h}{8e^2} = \frac{1}{4} Z_{c,\text{C.M.}} \tag{45}$$

For the circuit model where we terminate the end of the transmission line with a contact impedance equal to half the total dc resistance, we assume that each of the four transmission lines has a resistance at each end equal to $h/2e^2$. Therefore, by the definition of the common mode transmission line parameters, we need to use a load impedance of $Z_L = h/8e^2$ in (41) in order to implement the model discussed in the first paragraph of this section.

In the second step of the calculation, we note that the total impedance is just the contact resistance of the left-hand side of the nanotube plus the input impedance of (38). If we take the contact resistance on each side to be half of the total dc resistance (i.e., $R_{\text{contact}} = h/8e^2$), then we have the desired result

$$Z_{\text{nanotube}} = \frac{h}{8e^2} + Z_{c,\text{effective}} \frac{1 + \Gamma e^{-2\gamma l}}{1 - \Gamma e^{-2\gamma l}}. \tag{46}$$

This is a clear prediction that can be experimentally measured. While it may seem like a complicated result, it is actually quite elegant. What is more, we recently verified experimentally the 2-D analog of (46) in [12].

Before we turn to a numerical evaluation of (46), let us consider qualitatively the expected frequency-dependent behavior. At low frequencies, we should recover the dc limit of a real impedance of $h/4e^2$. This can indeed be shown to be the case, by taking the $\omega \to 0$ limit of (46). As the frequency is increased (assuming the damping is not too severe, see below), there will be resonant peaks in Z_{nanotube} as a function of frequency, corresponding to first, second, third, etc., harmonic of the fundamental wave vector set by the finite length of the tube. Applying this high-frequency voltage would *directly* excite the 1-D Lüttinger liquid low-energy excitations (the 1-D plasmons). The locations of these peaks in frequency space can be used to determine the wave velocity of this mode and, hence, g.

D. Numerical Evaluation of Impedance Versus Frequency

At this point, the best way to proceed is to evaluate (46) numerically for some possibly typical cases, which leads into the discussion of the numerical value of the distributed resistance $\mathcal{R}$ which (in addition to the contact resistance) causes damping. This discussion must be somewhat speculative, since the 1-D plasmon damping has never been measured, in fact the 1-D plasmon itself has not yet been directly observed. Currently very little is known about possible mechanisms. Our model of a distributed resistance per unit length gives rise to an exponential decay in a propagating 1-D plasmon wave, with a decay length given by

$$l_{\text{decay}} = \frac{2Z_{c,\text{effective}}}{\mathcal{R}}. \tag{47}$$

(We implicitly assume the limit $\omega > \mathcal{R}/\mathcal{L}_{\text{eff}}$ in (47). The more general case will be discussed below.) Before we discuss estimates for the numerical value of $\mathcal{R}$, we discuss what effect it would have on the plasmon resonance discussed above. As microwave engineers intuitively know, when the length of the transmission line (in this case nanotube) is much longer that the decay length l_{decay}, there is no resonant behavior to the transmission line, and the input impedance becomes the characteristic impedance of the transmission line Z_c, independent of the "load" impedance. Physically, this is because the wave that propagates toward the load gets essentially completely attenuated before it reaches the load. On the other hand, if the transmission line is shorter than the decay length l_{decay}, then the impedance becomes resonant as in the case we discussed above, with some damping, hence, finite Q.

In the absence of either theory or data, we conjecture that the decay length scale for 1-D Lüttinger liquid plasmons must be at least as long as the mean free path determined from dc transport measurements. Since the mean free path is known to be at least 1 μm long, the resistance per length is less than 25 kΩ/μm [using (47)]. Another technique to estimate an upper limit on $\mathcal{R}$ is to use data from recent STM experiments [40] which measure the voltage drop along the length of the tube for *semiconducting* tubes. There, the resistance per unit length is found to be 9 kΩ/μm. (Presumably, metallic tubes have an even lower resistance per unit length.) In this (presumably worst case) scenario, the damping length l_{decay} would be equal to roughly 3 μm. We

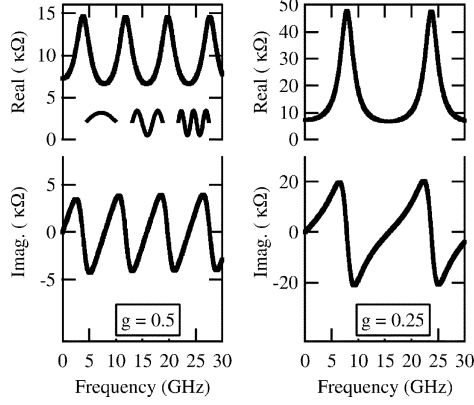Fig. 8. Predicted nanotube dynamical impedance for ohmic contact, for two different values of g. We assume $l = 100\mu m$.

Fig. 9. Predicted nanotube dynamical impedance in overdamped case.

consider below two important cases in turn: first, where the tube length is less than l_{decay}, hence, resonator $Q > 1$, and second in the "overdamped" limit where the tube length is greater than l_{decay}, hence, resonator $Q < 1$.

For the case of tube lengths less than the decay length, we discuss nanotubes of length 100 μm. Recent progress on CVD growth [26] has made such long SWNTs possible. With such a long length, the resonance frequencies will be in the gigahertz (GHz) range, where experiments are feasible. In the THz frequency range, it should also be possible to measure frequency-dependent properties [15], [16], which would be relevant for tubes with lengths in the μm range. The technical challenges in the THz range are not straightforward, though, and generally more difficult than in the GHz range. Since we have had excellent experimental success with measuring 2-D plasmons [12] in the GHz range, that is where we focus our attention. However, our predictions should also apply to THz resonance frequency experiments.

We chose (optimistically) a resistance per unit length of 10 Ω/μm, which is much less than the experimental upper limit of 10 kΩ/μm. In the case that the total resistance distributed along the length of the nanotube (i.e. $\mathcal{R} * l$) is less than the contact resistance, the resistance of the contacts is the dominant damping mechanism. This is the case for the parameters we have chosen. We plot in Fig. 8 the predicted nanotube dynamical impedance, for two different values of g. The predicted value of g is 0.25, and we also plot the predicted value of Z_{nanotube} for g = 0.5, which we achieve by numerically adjusting C_{ES} in our model. It is clear from Fig. 8 that it is still possible to have Q factors greater than 1, even when the contact resistance is much larger than the distributed "channel" resistance. Thus, the contact resistance causes damping but does not necessarily cause Q to be less than 1. Hence, it is still possible to observe the features of the Lüttinger liquid even in the presence of the contact resistance.

In principle, it should be possible to build a measurement apparatus that could measure this prediction. There are two main technical challenges. First, the impedance is high, which is difficult for microwave experiments to resolve. This issue could be solved by measuring many nanotubes of the same length in parallel, although one would need to assume that each tube had the same g factor, damping, etc. The second challenge is that
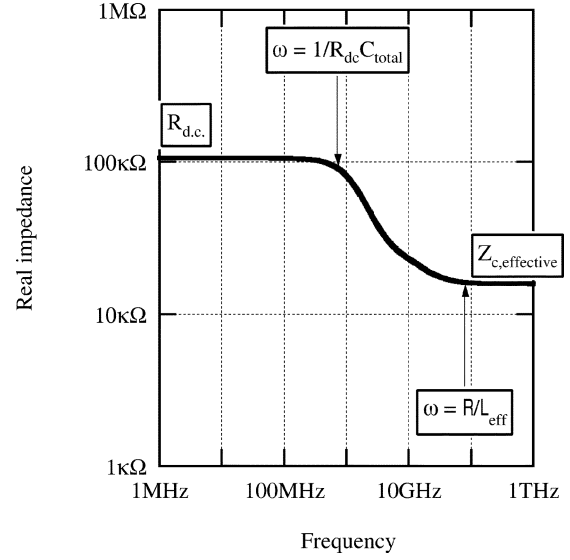
the macroscopic lead will have a finite capacitance to ground, just by virtue of the fact that the lead is finite in size. This capacitance to ground in many conceivable geometries will provide a low-impedance path to ground in parallel with the high-impedance nanotube, which will effectively short the nanotube to ground. This second difficulty makes the "ohmically" contacted geometry very difficult to realize experimentally. However, with sufficient effort it should be feasible.

An interesting prediction of our model is the frequency at which the first resonance occurs. The real part of the impedance peaks at a quarter wavelength. (It is a general result from microwave and RF engineering that the quarter wavelength structures transform open circuits to short circuits and vice versa. This fact is used in many modern RF circuits.) The resonance frequency can be written as

$$f_{\text{resonance}} = \frac{v_F}{4L}\frac{1}{g}. \tag{48}$$

At this frequency, the imaginary part of the impedance crosses zero. Therefore, if a measurement scheme can be devoiced to measure the where the imaginary part of the ohmically contacted nanotube impedance changes sign, this would be a *direct* measurement of the Lüttinger liquid parameter g, since L and v_F would be known. An additional interesting parameter is the equation of the Q of the resonance. This can be estimated as

$$Q = \frac{Z_{c,\text{effective}}}{2R_{\text{total}}} \tag{49}$$

where R_{total} is the total resistance of the nanotube.

We now consider the opposite case, that of an "overdamped" 1-D plasmon. We consider again a tube of length 100 μm, and now we consider resistance per unit length of 1 kΩ/μm. In this case, there will be no resonant frequency behavior. We plot in Fig. 9 the predicted real impedance [using (46)] for these parameters, assuming g = 0.25. There are two qualitative features that we would like to discuss. First, at dc the real impedance is simply the resistance per length times the length, i.e., $\mathcal{R}l$. As the
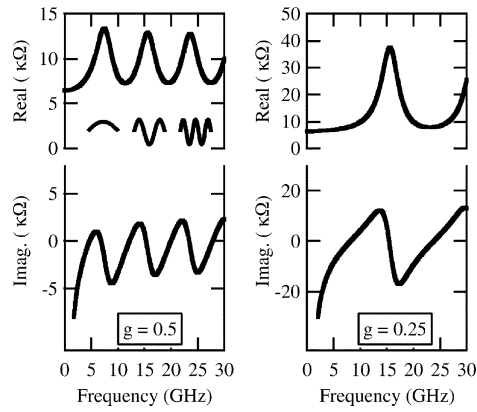
Fig. 10.   Predicted nanotube dynamical impedance for ohmic contact on one end only for two different values of g.

frequency is increased, the impedance falls. The frequency scale at which the impedance starts to change is given by the inverse of the total capacitance ($\mathcal{C}_{\mathrm{eff}}l$) times the total resistance. At very high frequencies, the impedance becomes equal to the effective characteristic impedance given in (40). The frequency at which this occurs is given by the inverse of the effective "L/R" time constant, which is the resistance per unit length divided by the inductance per unit length. We note that in this high frequency limit, the effective characteristic impedance ($Z_{c,\mathrm{eff}}$) given by (40) is mostly real. Therefore, even in the overdamped case where there is no resonant behavior, the transmission-line behavior of the nanotube becomes important at frequencies below 1 GHz.

E. Ohmic Contacted Resonance Measurement on One End

Another possible measurement setup would consist of making electrical contact on one end only of the nanotube, and letting the other end "float." This would correspond to cutting the wire to ground on the right-hand side of Fig. 7. At dc, no current would flow so the impedance would be infinite. However, at ac current could flow in and out of the end of the tube (charging and discharging the capacitors), so it is still meaningful to consider the dynamical impedance. In this case, we can still use (46) to predict this dynamical impedance, with a "load" impedance in equation (41) of infinity (corresponding to an open circuit at the other end of the nanotube.) We plot in Fig. 10 the predicted dynamical impedance in this case, where we have again assumed a length of 100 μm, but where we use a resistance per unit length of 100 Ω/μm. Resonant behavior is still predicted, but now the first peak in the real impedance occurs at half a wavelength.

F. Capacitively Contacted Measurement

The fabrication of electrical contacts to carbon nanotubes with low resistance at dc is not a trivial challenge. Even if it can be achieved, the "contact" resistance at ac may be different than it is at dc for unknown physics reasons. An alternative approach would be to use capacitive contacts to the nanotube. In the context of the above discussion, it should be clear that there is already capacitive coupling between the ground plane and the nanotube, so how can one achieve capacitive coupling to a macroscopic lead?

One solution is simply to turn the problem upside down. We envisage laying a carbon nanotube on an *insulating* substrate, and then evaporating a metallic, macroscopic lead onto the top of one end of the nanotube, and another macroscopic, metallic lead onto the top of the other end of the nanotube. One lead is connected to ground, and the other lead is connected to an ac voltage source. The impedance from one lead to the other is measured. This corresponds to measuring the impedance from one lead to the nanotube plus the impedance from the nanotube to the other lead. By the symmetry in the problem, we only need to consider one of those impedances and multiply by two. The effective circuit diagram we consider is shown in Fig. 11. The physical geometry is indicated schematically in Fig. 12. This capacitive coupling scheme is exactly the scheme we used for capacitive coupling to 2-D plasmons; see [12, Fig. 2].

Now, let us consider the impedance from one lead to the nanotube. It should be obvious by now that the capacitive contact cannot be treated as a lumped capacitance. Rather, the capacitance between the lead and the nanotube is distributed along the length of the tube. We must also keep in mind that there is a distributed kinetic inductance along the length of the tube. This may seem like a difficult problem, but in fact we have already developed the mathematical machinery necessary to fully solve this problem. The impedance from the macroscopic lead to the nanotube is equal to the impedance from the nanotube to the lead. Above, we calculated the impedance from a nanotube to "ground." In the case we are considering here we can use the results of those calculations, only now instead of the nanotube coupled to a ground plane, it is coupled to a lead. Thus, the impedance of the capacitive coupling to the nanotube is exactly equal to the impedance calculated in (38), with Z_L equal to infinity. Therefore, the impedance from one lead to another is equal to twice the impedance of (38). We calculate this numerically and plot the result in Fig. 13, for a tube length of 100 μm under each lead, and a very short length of nanotube between the leads. We use a resistance per length of 100 Ω/μm. The resonant behavior is again clear. This technique may be conceptually the most difficult to understand, but is in practice the simplest to implement experimentally.

G. Quantum Electric Field Effects

In the above calculations the electromagnetic field is considered classical. However, at low (and even room [41]) temperatures the capacitive charging energy can be considered quantized since $e^2/2C$ can be much less than k_BT. Additionally, the electromagnetic field must be considered quantum mechanically (as photons) if the photon energy $h\nu$ is greater than the charging energy. This occurs as a typical energy of 0.5 K for a 10-GHz photon. Therefore, if the discreteness of the photon field is taken into account, a more sophisticated quantum treatment of the nanotube dynamical impedance, which takes into account processes such as photon assisted tunneling, will be necessary. Such a treatment is beyond the scope of this paper.

H. RF Nano-Spintronics

Finally, we mention here briefly that a similar set of calculations can be performed [42] to predict the dynamical *spin*
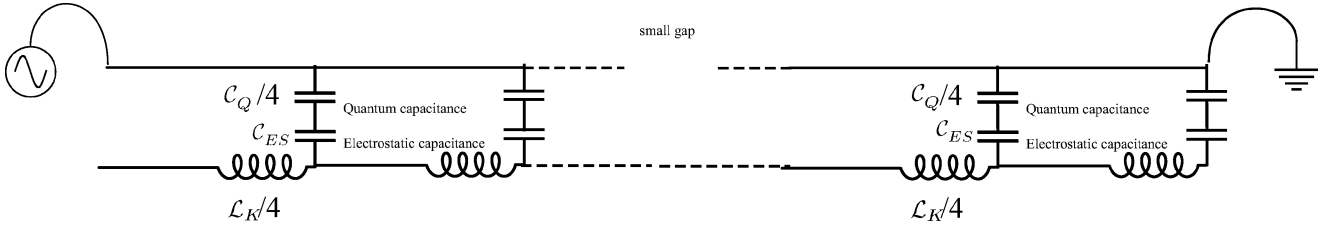
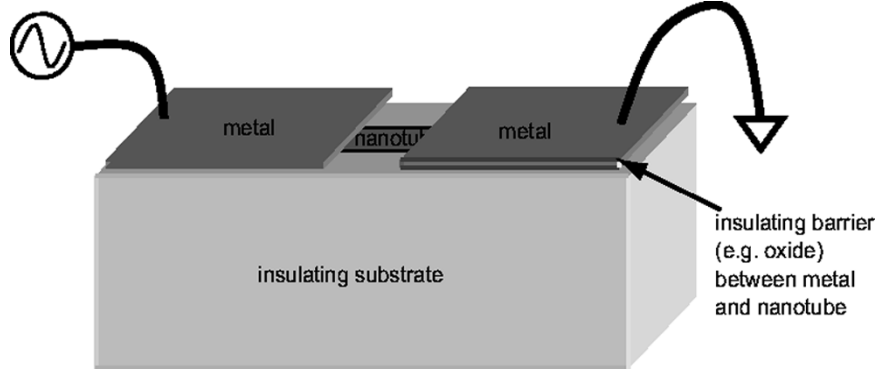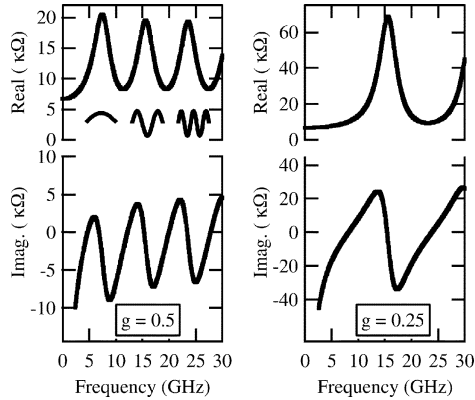Fig. 11.   Circuit diagram for capacitively coupled nanotube.

Fig. 12.   Geometry for capacitive contact. The spacing between the metal electrodes has been enlarged for clarity. No dc electrical contact to the nanotube is implied in this picture, only capacitive coupling to the leads.

Fig. 13.   Predicted nanotube dynamical impedance for capacitive contact on one end for two different values of g.

impedance of a SWNT. This could open up a new area of research into RF spin-polarized transport in 1-D systems for applications in "nano-spintronics."

V. CONCLUSIONS

We have considered the dynamical properties of single-walled carbon nanotubes from a circuit point of view. The 1-D plasmon should be observable using the same experimental technique we developed for measurements of the 2-D plasmons. This measurement would be direct confirmation of Lüttinger liquid behavior of a 1-D system of interacting quantum particles. We have formulated our experimental technique and predictions in the frequency domain, but it should also be possible to perform a time domain experiment using similar principles to measure the wave velocity and damping. Finally, the RF circuit models we have presented here provide

the foundation for our current research aimed at active nanotube *transistors* with switching speeds approaching the THz range.

APPENDIX

We now proceed mathematically to solve for the normal modes. The charge per unit length of the ith mode is related to the voltages of the four other modes, which (upon inspection of the circuit diagram in Fig. 4 we write as a matrix generalization of $Q = \mathbf{C}V$

$$
\begin{pmatrix}
V_{a\uparrow}(x,t) \\
V_{a\downarrow}(x,t) \\
V_{b\uparrow}(x,t) \\
V_{b\downarrow}(x,t)
\end{pmatrix}
$$
$$
= \begin{pmatrix}
\mathcal{C}_Q^{-1}+\mathcal{C}_{ES}^{-1} & \mathcal{C}_{ES}^{-1} & \mathcal{C}_{ES}^{-1} & \mathcal{C}_{ES}^{-1} \\
\mathcal{C}_{ES}^{-1} & \mathcal{C}_Q^{-1}+\mathcal{C}_{ES}^{-1} & \mathcal{C}_{ES}^{-1} & \mathcal{C}_{ES}^{-1} \\
\mathcal{C}_{ES}^{-1} & \mathcal{C}_{ES}^{-1} & \mathcal{C}_Q^{-1}+\mathcal{C}_{ES}^{-1} & \mathcal{C}_{ES}^{-1} \\
\mathcal{C}_{ES}^{-1} & \mathcal{C}_{ES}^{-1} & \mathcal{C}_{ES}^{-1} & \mathcal{C}_Q^{-1}+\mathcal{C}_{ES}^{-1}
\end{pmatrix}
$$
$$
\begin{pmatrix}
\rho_{a\uparrow}(x,t) \\
\rho_{a\downarrow}(x,t) \\
\rho_{b\uparrow}(x,t) \\
\rho_{b\downarrow}(x,t)
\end{pmatrix}. \tag{50}
$$

(This is equivalent to [19, eq. (24)].) We write this in vector notation as

$$
\vec{V}(x,t) = \mathbf{C}^{-1}\vec{\rho}(x,t). \tag{51}
$$

At this point, we can follow the derivation of the telegrapher equations, using the matrix generalization. Kirchoff's voltage law gives

$$
\frac{\partial \vec{V}(x,t)}{\partial x} = -\mathcal{L}_K \frac{\partial \vec{I}(x,t)}{\partial t}. \tag{52}
$$

(This can be seen by considering the voltage just to the left and just to the right of any of the inductors drawn in Fig. 4). In the derivation of the telegrapher equations, Kirchoff's current law is usually used. It is easier in this case to use the continuity equation, which in one dimension is given by

$$\frac{\partial \vec{\rho}(x,t)}{\partial t} = -\frac{\partial \vec{I}(x,t)}{\partial x}. \tag{53}$$

We now proceed to take the second time derivative of (51), yielding

$$\frac{\partial}{\partial t}\frac{\partial}{\partial t}\vec{V}(x,t) = \frac{\partial}{\partial t}\mathbf{C}^{-1}\frac{\partial \vec{\rho}(x,t)}{\partial t} = -\mathbf{C}^{-1}\frac{\partial}{\partial t}\frac{\partial \vec{I}(x,t)}{\partial x}$$

$$= -\mathbf{C}^{-1}\frac{\partial}{\partial x}\frac{\partial \vec{I}(x,t)}{\partial t}$$

$$= -\mathbf{C}^{-1}\frac{\partial}{\partial x}\frac{1}{\mathcal{L}_k}\frac{\partial \vec{V}(x,t)}{\partial x}. \tag{54}$$

In sum,

$$\frac{\partial^2 \vec{V}(x,t)}{\partial t^2} = \frac{\mathbf{C}^{-1}}{\mathcal{L}_{\mathcal{K}}}\frac{\partial^2 \vec{V}(x,t)}{\partial x^2}. \tag{55}$$

Using the same methods it can be shown that

$$\frac{\partial^2 \vec{I}(x,t)}{\partial t^2} = \frac{\mathbf{C}^{-1}}{\mathcal{L}_{\mathcal{K}}}\frac{\partial^2 \vec{I}(x,t)}{\partial x^2}. \tag{56}$$

Thus, we have a set of four coupled wave equations for the voltage and current on each line.

Finally, there exists a matrix relating $\overrightarrow{V}(x,t)$ and $\overrightarrow{I}(x,t)$, the impedance matrix. This is discussed in [19] in this basis. We do not consider the impedance matrix in this basis here, as it is not relevant to the experimental setup we discuss below. In contrast to [19], we will discuss the impedance in a different basis, where it is diagonal.

Let us consider the voltage wave equation (55). If $\mathcal{C}_{ES} = 0$, then $\mathbf{C}$ is diagonal, and the voltage wave (plasmon) in each mode is independent of the others, all moving at the Fermi velocity. If $\mathcal{C}_{ES}$ is nonzero, this is tantamount to saying there are interactions, and the four modes are coupled. We need now to diagonalize the equations of motion to find the normal modes. If we want to consider solutions of the form

$$\vec{V}(x,t) = \vec{V}_0 e^{i(kx - \omega t)} \tag{57}$$

then we must find which values of $\vec{V}_0$ will work solve the coupled wave equations (55) and (56). In other words, we need to find a set of vectors which diagonalizes the capacitance matrix. Specifically, we must solve (on plugging the above (57) into the voltage wave equation (55))

$$\frac{\omega^2}{k_2}\vec{V}_0 = \frac{\mathbf{C}^{-1}}{\mathcal{L}_{\mathcal{K}}}\vec{V}_0. \tag{58}$$

(This is equivalent to [19, eq. (27)], which, in turn, is equivalent to [29, eq. (11)].)The eigenvectors are

$$\vec{V}_0 = \overset{\text{C.M.}}{\begin{pmatrix}1\\1\\1\\1\end{pmatrix}}, \overset{D1}{\begin{pmatrix}1\\1\\-1\\-1\end{pmatrix}}, \overset{D2}{\begin{pmatrix}1\\-1\\1\\-1\end{pmatrix}}, \overset{D3}{\begin{pmatrix}1\\-1\\-1\\1\end{pmatrix}}. \tag{59}$$

We have labeled the eigenvectors C.M. for "common mode" and $D1$–$D3$ for differentials 1–3. The "common-mode" vector is the fundamental charged excitation in a Lüttinger liquid. Below, we discuss a method to excite these modes with a microwave voltage. The other three are neutral, that is, they carry no net (charge) current. (Since the other three are degenerate, it is possible to chose a different basis for the other three. A basis of nonorthogonal degenerate eigenvectors was used in [19], but we chose the orthogonal eigenvectors as in [43], [44], and [30].) However, the differential modes do carry *spin* current. These are the neutral and charged modes of a Lüttinger liquid. This is the clear separation of spin and charge degrees of freedom which is the hallmark of a Lüttinger liquid.

In the new basis, the capacitance matrix is diagonal. If we write the voltages in the new basis as

$$\vec{V}_0'(x,t)$$
$$= \begin{pmatrix} V_{\text{C.M.}}(x,t) \\ V_{D1}(x,t) \\ V_{D2}(x,t) \\ V_{D3}(x,t) \end{pmatrix}$$
$$= \begin{pmatrix} V_{a\uparrow}(x,t) + V_{a\downarrow}(x,t) + V_{b\uparrow}(x,t) + V_{b\downarrow}(x,t) \\ V_{a\uparrow}(x,t) + V_{a\downarrow}(x,t) - V_{b\uparrow}(x,t) - V_{b\downarrow}(x,t) \\ V_{a\uparrow}(x,t) - V_{a\downarrow}(x,t) + V_{b\uparrow}(x,t) - V_{b\downarrow}(x,t) \\ V_{a\uparrow}(x,t) - V_{a\downarrow}(x,t) - V_{b\uparrow}(x,t) + V_{b\downarrow}(x,t) \end{pmatrix} \tag{60}$$

and similarly for $\overrightarrow{\rho}_0(x,t)$ and $\overrightarrow{I}_0(x,t)$, then the new capacitance matrix is simply given by

$$\begin{pmatrix} V_{\text{C.M.}}(x,t) \\ V_{D1}(x,t) \\ V_{D2}(x,t) \\ V_{D3}(x,t) \end{pmatrix} = \begin{pmatrix} C_Q^{-1} + 4C_{ES}^{-1} & 0 & 0 & 0 \\ 0 & C_Q^{-1} & 0 & 0 \\ 0 & 0 & C_Q^{-1} & 0 \\ 0 & 0 & 0 & C_Q^{-1} \end{pmatrix}$$
$$= \begin{pmatrix} \rho_{\text{C.M.}}(x,t) \\ \rho_{D1}(x,t) \\ \rho_{D2}(x,t) \\ \rho_{D3}(x,t) \end{pmatrix} \tag{61}$$

or, in vector notation,

$$\overrightarrow{V}'(x,t) = \boldsymbol{C}'^{-1}\overrightarrow{\rho}'(x,t). \tag{62}$$

Additionally, in the new basis the following holds:

$$\frac{\partial \overrightarrow{V}'(x,t)}{\partial x} = -\mathcal{L}_{\mathcal{K}}\frac{\partial \overrightarrow{I}'(x,t)'}{\partial t} \tag{63}$$

and

$$\frac{\partial \overrightarrow{\rho}'(x,t)}{\partial t} = -\frac{\partial \overrightarrow{I}'(x,t)}{\partial x}. \tag{64}$$

In this new basis, the wave equation for the voltage is now diagonal, with new wave equations given by

$$\frac{\partial^2 V_{CM}(x,t)}{\partial t^2} = \frac{1}{\mathcal{L}_{\mathcal{K}}}\left(\frac{1}{C_Q} + \frac{4}{C_{ES}}\right)\frac{\partial^2 V_{CM}(x,t)}{\partial x^2} \tag{65}$$

$$\frac{\partial^2 V_{D1}(x,t)}{\partial t^2} = \frac{1}{C_Q \mathcal{L}_{\mathcal{K}}}\frac{\partial^2 V_{D1}(x,t)}{\partial x^2} \tag{66}$$

with the equation for $D2$ and $D3$ the same as for D1. In vector form

$$\frac{\partial^2 \overrightarrow{V}'(x,t)}{\partial t^2} = \frac{C'^{-1}}{\mathcal{L}_{\mathcal{K}}}\frac{\partial^2 \overrightarrow{V}'(x,t)}{\partial x^2}. \tag{67}$$

Similarly, one can show that

$$\frac{\partial^2 \overrightarrow{I}'(x,t)}{\partial t^2} = \frac{C'^{-1}}{\mathcal{L}_{\mathcal{K}}}\frac{\partial^2 \overrightarrow{I}'(x,t)}{\partial x^2}. \tag{68}$$

Now, the wave velocity for the differential modes is just the Fermi velocity (using (66) above). However, the velocity for the common mode, i.e., 1-D plasmon, is given by

$$v_p = \sqrt{\frac{1}{\mathcal{L}_{\mathcal{K}}}\left(\frac{1}{C_Q} + \frac{4}{C_{ES}}\right)} = v_F\sqrt{1 + \frac{4C_Q}{C_{ES}}} \equiv v_F/g. \tag{69}$$

This equation (which is not a new result [1]) defines g for an SWNT. Now, let us consider solutions to the voltage and current wave equations in the diagonal basis, in order to determine the characteristic impedance. Since the wave equations are diagonal (i.e., uncoupled), if we can excite the common mode, none of the other modes will be excited.

The general solutions are of the form

$$V_{\text{C.M.}}(x,t) = V_{C.M}^+ e^{i(kx-wt)} + V_{\text{C.M.}}^- e^{i(-kx+wt)} \tag{70}$$

and

$$I_{\text{C.M.}}(x,t) = I_{\text{C.M.}}^+ e^{i(kx-wt)} + I_{\text{C.M.}}^- e^{i(-kx-wt)}. \tag{71}$$

Applying (63) to (71) for the current gives the following:

$$I_{\text{C.M.}}(x,t) = \sqrt{\frac{4\mathcal{L}_{\mathcal{K}}}{C_{ES}} + \frac{\mathcal{L}_{\mathcal{K}}}{C_q}}$$
$$\times\left(V_{\text{C.M.}}^+ e^{i(kx-wt)} - V_{\text{C.M.}}^- e^{i(-kx+wt)}\right). \tag{72}$$

The ratio of the ac voltage to the ac current on the line is defined as the "characteristic impedance," which can be seen from

comparing (72) to (70). Thus, for the common mode, the characteristic impedance is given by

$$Z_{c,\text{C.M.}} \equiv \frac{V_{\text{C.M.}}^+}{I_{\text{C.M.}}^+} = -\frac{V_{\text{C.M.}}^-}{I_{\text{C.M.}}^-} = \sqrt{\frac{4\mathcal{L}_{\mathcal{K}}}{C_{ES}} + \frac{\mathcal{L}_{\mathcal{K}}}{C_Q}} = \frac{1}{g}\frac{h}{2e^2}. \tag{73}$$

This is a very important number which will be used in the experimental techniques section to be discussed below. Our result differs from [19, eq. (37)] because we are considering the excitation of only the common mode, i.e., Lüttinger liquid charge mode. Reference [19] considered the excitation of mode $V_{a\uparrow}$, i.e., a superposition of charge and spin modes. Below we discuss how our method excites only the charge mode, and not the spin mode, so that our calculation is more germane to our experimental technique described below to directly excite Lüttinger liquid collective modes.

Now, it is important to realize that what one measures is not exactly Z_c for the common mode. The common mode impedance is the sum of the voltages $(V_{a,\uparrow} + V_{a,\downarrow} + V_{b,\uparrow} + V_{b,\downarrow})$ divided by the sum of the currents $(I_{a,\uparrow} + I_{a,\downarrow} + I_{b,\uparrow} + I_{b,\downarrow})$. The sum of the currents is what flows into an external circuit. However, when coupled to an external circuit all of the voltages are equal to the eternally measured voltage, so that the common mode voltage is actually four times larger than the voltage measured at the end of the tube by an external circuit. That is why our (73) differs from [18, eq. (3)].

Finally, for the sake of completeness, it can be shown that the following is the characteristic impedance of the other three modes:

$$Z_{c,D1} \equiv \frac{V_{D1}}{I_{D1}} = \sqrt{\frac{\mathcal{L}_{\mathcal{K}}}{C_Q}} = \frac{h}{2e^2}. \tag{74}$$

This describes the ratio of the voltage to the current when the spin wave is excited.

ACKNOWLEDGMENT

REFERENCES

[1] M. P. A. Fisher and L. I. Glazman, "Transport in a one-dimensional Lüttinger liquid," in *Mesoscopic Electron Transport*. Dordrecht, The Netherlands: Kluwer, 1997.

[2] Ph. Avouris, M. S. Dresselhaus, and G. Dresselhaus, Eds., *Carbon Nanotubes: Synthesis, Structure, Properties, and Applications*. Berlin, Germany: Springer-Verlag, 2001, vol. 80, Topics in Applied Physics.

[3] S. Tomonaga, "Remarks on Bloch's method of sound waves applied to many-Fermion problems," *Prog. Theor. Phys.*, vol. 5, no. 4, pp. 544–569, 1950.

[4] J. M. Lüttinger, "An exactly solvable model of a many-Fermion system," *J. Math. Phys.*, vol. 4, no. 9, p. 1154, 1963.

[5] A. O. Gogolin, A. A. Nersesyan, and A. M. Tsvelik, *Bosonization and Strongly Correlated Systems*. Cambridge, U.K.: Cambridge Univ. Press, 1998.

[6] G. D. Mahan, *Many-Particle Physics*, 2nd ed. New York: Plenum, 1990.

[7] F. D. M. Haldane, "Effective harmonic-fluid approach to low-energy properties of one-dimensional quantum fluids," *Phys. Rev. Lett.*, vol. 47, no. 25, pp. 1840–1843, Dec. 1981.

[8] M. Bockrath, D. H. Cobden, J. Lu, A. G. Rinzler, R. E. Smalley, L. Balents, and P. L. McEuen, "Lüttinger-liquid behavior in carbon nanotubes," *Nature*, vol. 397, pp. 598–601, 1999.

[9] V. V. Ponomarenko, "Frequency dependences in transport through a Tomonaga-Lüttinger liquid wire," *Phys. Rev. B*, vol. 54, no. 15, pp. 10 328–10 331, Oct. 1996.

[10] V. A. Sablikov and B. S. Shchamkhalova, "Dynamic conductivity of interacting electrons in open mesoscopic structures," *JETP Lett.*, vol. 66, no. 1, pp. 41–46, July 1997.

[11] Y. M. Blanter, F. W. J. Hekking, and M. Büttiker, "Interaction constants and dynamic conductance of a gated wire," *Phys. Rev. Lett.*, vol. 81, no. 9, pp. 1925–1928, Oct. 1998.

[12] P. J. Burke, I. B. Spielman, J. P. Eisenstein, L. N. Pfeiffer, and K. W. West, "High frequency conductivity of the high-mobility two-dimensional electron gas," *Appl. Phys. Lett.*, vol. 76, no. 6, pp. 745–747, Feb. 2000.

[13] O. M. Auslaender, A. Yacoby, R. de Picciotto, K. W. Baldwin, L. N. Pfeiffer, and K. W. West, "Tunneling spectroscopy of the elementary excitations in a one-dimensional wire," *Science*, vol. 295, pp. 825–828, 2002.

[14] P. J. Burke and J. P. Eisenstein. (1998, Aug.) Interlayer plasmons. [Online] Available: http://nano.ece.uci.edu

[15] X. G. Peralta, S. J. Allen, N. E. Harff, M. C. Wanke, M. P. Lilly, J. A. Simmons, J. L. Reno, P. J. Burke, and J. P. Eisenstein, "Terahertz photoconductivity and plasmon modes in double quantum well field effect transistors," *Appl. Phys. Lett.*, vol. 81, no. 9, pp. 1627–1629, Aug. 2002.

[16] X. G. Peralta, "Terahertz photoconductivity and plasmon modes in double-quantum-well field-effect transistors," Ph.D. dissertation, Univ. California, Santa Barbara, CA, 2002.

[17] M. W. Bockrath, "Carbon nanotubes: electrons in one dimension," Ph.D. dissertation, Univ. California, Berkeley, CA, 1999.

[18] R. Tarkiainen, M. Ahlskog, J. Pentillä, L. Roschier, P. Hakonen, M. Paalanen, and E. Sonin, "Multiwalled carbon nanotube: Lüttinger versus Fermi liquid," *Phys. Rev. B*, vol. 64, pp. 195412-1–195412-4, Oct. 2001.

[19] E. B. Sonin, "Tunneling into 1d and quasi-1d conductors and Lüttinger-liquid behavior," *J. Low Temp. Phys.*, no. 1, pp. 321–334, 2001.

[20] G. Cuniberti, M. Sassetti, and B. Kramer, "Transport and elementary excitations of a Lüttinger liquid," *J. Phys. C, Condens. Matter*, vol. 8, no. 2, pp. L21–L26, 1996.

[21] ——, "Ac conductance of a quantum wire with electron-electron interactions," *Phys. Rev. B*, vol. 57, no. 3, pp. 1515–1526, Jan. 1998.

[22] I. Safi and H. J. Schulz, "Transport in an inhomogeneous interacting one-dimensional system," *Phys. Rev. B*, vol. 52, no. 24, pp. 17040–17043, May 1995.

[23] V. A. Sablikov and B. S. Shchamkhalova, "Dynamic transport of interacting electrons in a mesoscopic quantum wire," *J. Low Temp. Phys.*, vol. 118, no. 5/6, pp. 485–494, 2000.

[24] M. Dyakonov and M. S. Shur, "Plasma wave electronics for terahertz applications," in *Terahertz Sources and Systems*. Boston, MA: Kluwer, 2001, vol. 27, NATO Science Series, II. Mathematics, Physics and Chemistry, pp. 187–207.

[25] S. Ramo, J. R. Whinnery, and T. Van Duzer, *Fields and Waves in Communication Electronics*. New York: Wiley, 1994.

[26] H. Dai, "Nanotube growth and characterization," in *Carbon Nanotubes Synthesis, Structures, Properties, and Applications*. Berlin, Germany: Springer-Verlag, 2001, vol. 80, Topics in Applied Physics.

[27] J. Kong, E. Yenilmez, T. W. Tombler, W. Kim, H. Dai, R. B. Laughlin, L. Liu, C. S. Jayanthi, and S. Y. Wu, "Quantum interference and ballistic transmission in nanotube electron waveguides," *Phys. Rev. Lett.*, vol. 87, no. 10, pp. 106801-1–106801-4, Sept. 2001.

[28] O. Hilt, H. B. Brom, and M. Ahlskog, "Localized and delocalized charge transport in single-wall carbon nanotube mats," *Phys. Rev. B*, vol. 61, no. 8, pp. 5129–5132, Feb. 2000.

[29] K. A. Matveev and L. I. Glazman, "Coulomb blockade of tunneling into a quasi-one-dimensional wire," *Phys. Rev. Lett.*, vol. 70, no. 7, pp. 990–993, Feb. 1993.

[30] C. Kane, L. Balents, and M. P. A. Fisher, "Coulomb interactions and mesoscopic effects in carbon nanotubes," *Phys. Rev. Lett.*, vol. 79, no. 25, pp. 5086–5089, Dec. 1997.

[31] L. Balents and R. Egger, "Spin transport in interacting quantum wires and carbon nanotubes," *Phys. Rev. Lett.*, vol. 85, no. 16, pp. 3464–3467, Oct. 2000.

[32] P. J. Burke, L. N. Pfeiffer, and K. W. West, "Effect of Nyquist noise on the Nyquist dephasing rate in two-dimensional electron systems," *Phys. Rev. B*, vol. 65, pp. 201310–201313, May 2002.

[33] A. A. Kozhevnikov, R. J. Schoelkopf, and D. E. Prober, "Observation of photon-assisted noise in a diffusive normal metal-superconductor junction," *Phys. Rev. Lett.*, vol. 84, no. 15, pp. 3398–3401, Apr. 2000.

[34] R. J. Schoelkopf, P. J. Burke, A. A. Kozhevnikov, and D. E. Prober, "Frequency dependence of shot noise in a diffusive mesoscopic conductor," *Phys. Rev. Lett.*, vol. 78, no. 17, pp. 3370–3373, Apr. 1997.

[35] J. B. Pieper and J. C. Price, "Frequency-dependence of h/e conductance oscillations in mesoscopic ag rings," *Phys. Rev. Lett.*, vol. 72, no. 22, pp. 3586–3589, May 1994.

[36] M. Büttiker and T. Christen, "Admittance and nonlinear transport in quantum wires, point contacts, and resonant tunneling barriers," in *Mesoscopic Electron Transport*. Dordrecht, The Netherlands: Kluwer, 1997.

[37] M. Büttiker, H. Thomas, and A. Prêtre, *Phys. Lett. A*, vol. 180, p. 364, 1993.

[38] P. Sheng, *Introduction to Wave Scattering, Localization, and Mesoscopic Phenomena*. San Diego, CA: Academic, 1995.

[39] D. M. Pozar, *Microwave Engineering*. New York: Wiley, 1998.

[40] P. L. McEuen, M. Fuhrer, and H. Park, "Single-walled carbon nanotube electronics," *IEEE Trans. Nanotechnol.*, vol. 1, pp. 78–85, Mar. 2002.

[41] H. W. C. Postma, T. Teepen, Z. Yao, M. Grifoni, and C. Dekker, "Carbon nanotube single-electron transistors at room temperature," *Science*, vol. 293, pp. 76–79, July 2001.

[42] P. J. Burke, unpublished.

[43] R. Egger and A. O. Gogolin, "Effective low-energy theory for correlated carbon nanotubes," *Phys. Rev. Lett.*, vol. 79, no. 25, pp. 5082–5085, Dec. 1997.

[44] R. Egger and A. O. Gogolin, "Correlated transport and non-Fermi-liquid behavior in single-wall carbon nanotubes," *Eur. Phys. J. B*, vol. 3, pp. 281–300, 1998.

P. J. Burke (M'97) received the Ph.D. degree in physics from Yale University, New Haven, CT, in 1998.

From 1998 to 2001, he was a Sherman Fairchild Postdoctoral Scholar in Physics at California Institute of Technology, Pasadena, where he studied resonant tunnel diodes for THz detectors and sources, 2-D plasmons, and the interaction between Johnson noise and quantum coherence in 2-D systems. Since 2001, he has been an Assistant Professor in the Department of Electrical and Computer Engineering, University of California, Irvine, where he is currently leading the initiative in nanotechnology. His research interests include nano-electronics, nano-mechanics, and nano-biotechnology, as well as quantum computation and quantum information processing.

Correspondence

Corrections to "An RF Circuit Model for Carbon Nanotubes"

P. J. Burke

In the above paper [1, eq. (14)], g should be replaced by g^{-1}. Thus, (14) should read

$$Z_{c,\text{interacting}} = \sqrt{\frac{\mathcal{L}_K}{\mathcal{C}_{\text{total}}}} = \sqrt{\frac{\mathcal{L}_K}{\mathcal{C}_{\text{ES}}} + \frac{\mathcal{L}_K}{\mathcal{C}_Q}} = g^{-1} \frac{h}{2e^2}.$$

The last sentence in Section III should read: In [11], we show that the circuit model of Fig. 1 is still valid as an effective circuit model for the charged mode if $\mathcal{L}_K$ is replaced by $\mathcal{L}_K/4$ and $\mathcal{C}_Q$ is replaced by $4\mathcal{C}_Q$.

REFERENCES

[1] P. J. Burke, "An RF circuit model for carbon nanotubes," *IEEE Trans. Nanotechnol.*, vol. 2, pp. 55–58, Mar. 2003.

Corrections to "Luttinger Liquid Theory as a Model of the Gigahertz Electrical Properties of Carbon Nanotubes"

P. J. Burke

In the above paper [1, p. 136], the equation appearing in the last line in the left-hand-side column should have read $(\mathcal{C}_{\text{ES}}^{-1} + (4\mathcal{C}_Q)^{-1})^{-1}$.

In the above paper [1], (43) should have read as follows:

$$\mathcal{C}_{\text{eff}}^{-1} = (4\mathcal{C}_Q)^{-1} + \mathcal{C}_{\text{ES}}^{-1}.$$

In the above paper [1], Figs. 5, 7, and 11 should have appeared as shown below in Figs. 1–3.

REFERENCES

[1] P. J. Burke, "Luttinger liquid theory as a model of the gigahertz electrical properties of carbon nanotubes," *IEEE Trans. Nanotechnol.*, vol. 1, pp. 129–144, Sept. 2002.
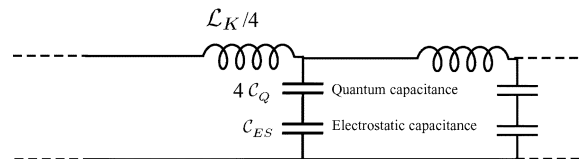
Fig. 1. Charge mode ("common mode") effective circuit diagram.
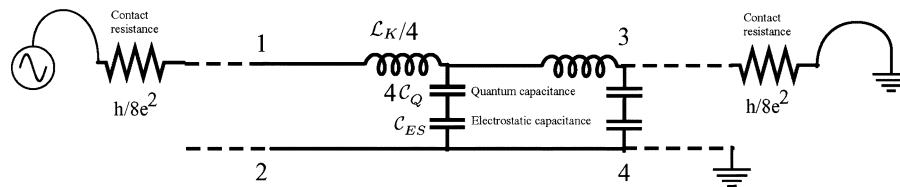

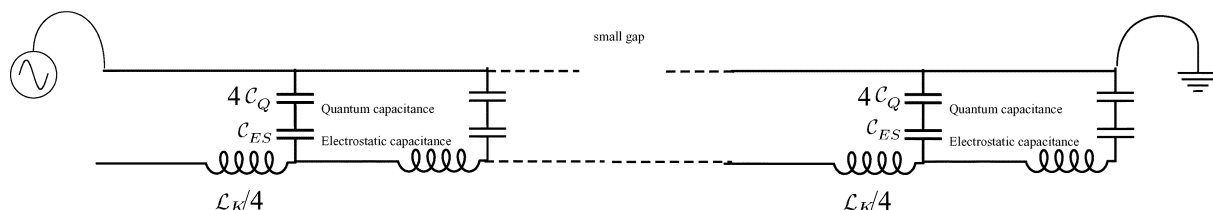Fig. 2. *Effective* circuit diagram for an SWNT with dc electrical contacts at both ends.

Fig. 3. Circuit diagram for capacitively coupled nanotube.